

“Iron Ion Relative Weathering Index”: A New Index for Identifying the Weathering Degree in Red Sandstone

Saidong Li,* Genlan Yang,* Wenjie Jiang, Xiqiong Xiang, and Chongping Huang

Cite This: *ACS Omega* 2024, 9, 10233–10242

Read Online

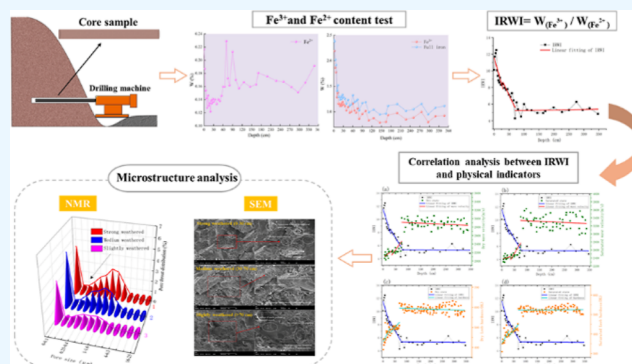
ACCESS |

Metrics & More

Article Recommendations

Supporting Information

ABSTRACT: The red bed region in west central and southern China is affected by hot and humid climate, where sandstone is intensely weathered. The weathered hazardous rocks seriously threaten the road and slope, making it challenging to protect the Danxia red bed. After considering the red sandstone's material composition and the local area's main weathering effects. We noticed that iron ions in red sandstone are susceptible to weathering, which leads to changes in the valence and content of iron ions. This study attempts to establish a new chemical weathering index called the “iron ion relative weathering index” (IRWI) to classify the weathering degree of red sandstone. This paper mainly explores the changes of physical characteristics (mineral composition, physical indicator, microstructure, and pore structure) from the surface to the interior of red sandstone in the actual environment and their correlation with IRWI. The study on the correlation between the physical indicators such as longitudinal wave velocity, resistivity, density, water absorption, and IRWI reveals that they have the same trends and are closely related to the weathering degree. The shallow weathering zone of Chishui red sandstone is divided into strong, medium, and slight weathering zones. Microscopically, the cementation and pore distribution of the red sandstone are consistent with the characteristics of the weathering zone. Therefore, IRWI not only is a reliable chemical quantitative method in indicating the weathering of red sandstone but also takes into account the controlling role of iron in the color development of red beds, which provides a new research idea for the quantitative identification of weathering degree and color mechanism of red sandstone.



1. INTRODUCTION

With the renewed global interest and increased focus on preserving the world's cultural heritage, sandstone has gradually become the focus of attention as a building material with good landscaping properties.¹ Most research on rock weathering and stone decay has focused on granite and limestone, while there is little research on the weathering of sandstone.² Determining the degree of rock weathering has undergone from qualitative to quantitative.³ According to the specification, the classification of rock weathering degree from a qualitative perspective (color, secondary minerals, degree of development of joints and fissures, degree of integrity, and hydrologic properties) has been widely recognized in engineering practice.⁴ However, diverse rock types and complex morphological changes after weathering make it vulnerable to human subjective factors, which leads to disagreement on the classification of rock weathering degree.⁵ Therefore, it is imperative to establish a simple and quantifiable weathering index or weathering degree evaluation standard. The hot and rainy weather of southwest China provides an environmental basis for weathering, and temperature change is considered as the main driving force for rock weathering.^{6–8} Temperature change is the main factor affecting the formation of Danxia landform.⁹ The cooling of sudden rainfall in a high-

temperature environment leads to the weathering fissures of red layer that can be generated under a day's thermal cycle.¹⁰ The humidity stress generated by water absorption under dry and wet cycles is the external dynamic factor controlling the differential weathering of red sandstone and conglomerate.¹¹ Under the influence of rain-heat cycle weathering all year round, a number of risk rocks have been developed in the Danxia area of Chishui. Weathering is an essential factor in destabilizing and spalling slope rock and a weak interlayer, so determining the weathering degree of Danxia red sandstone has become a primary concern. The weathering index, as a means of quantitative evaluation with the gain or loss of minerals, chemical composition content, is suitable for exploring weathering characteristics because of its strong operability and quantifiable characteristics.¹²

Received: September 25, 2023

Revised: January 26, 2024

Accepted: January 31, 2024

Published: February 21, 2024



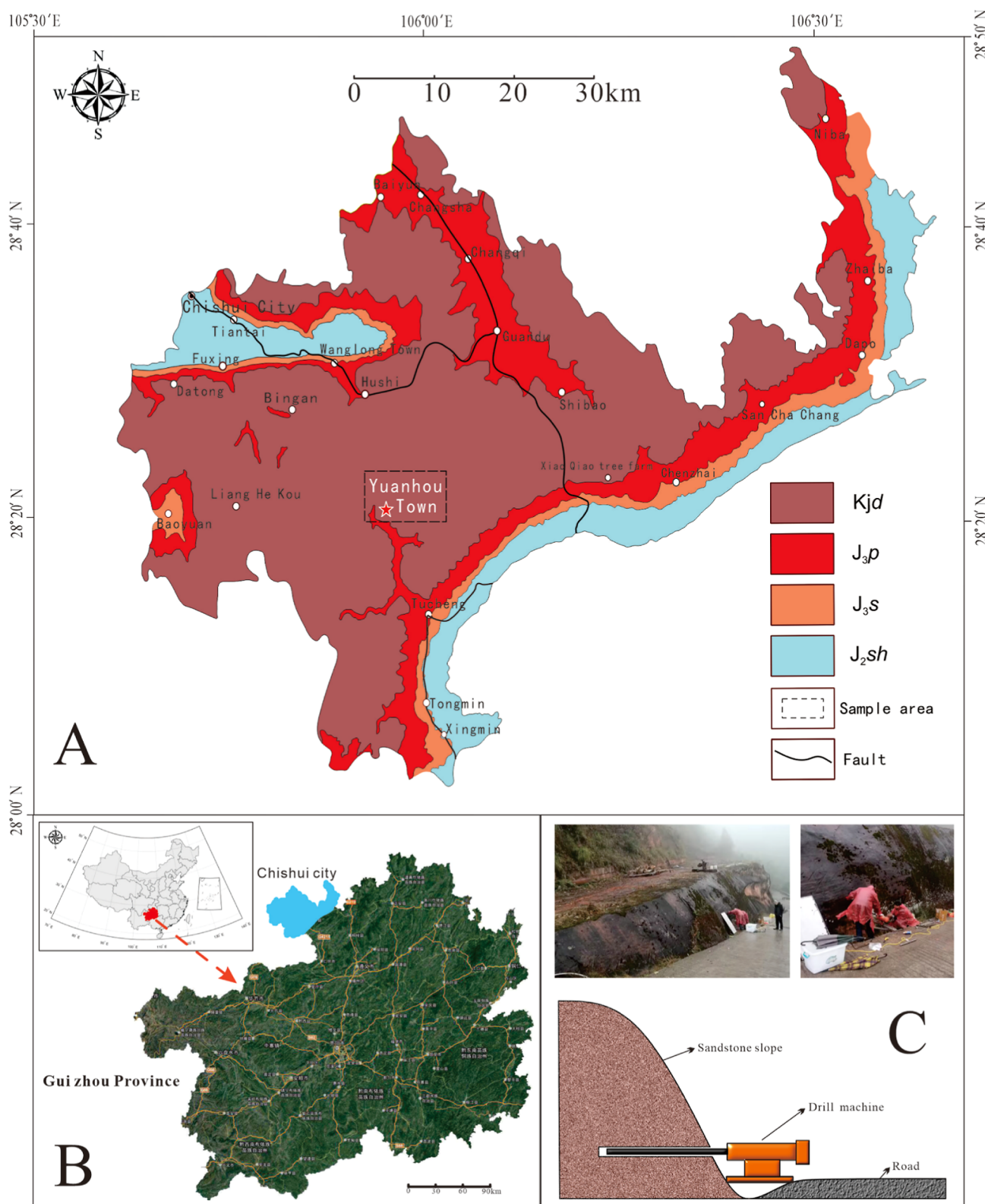
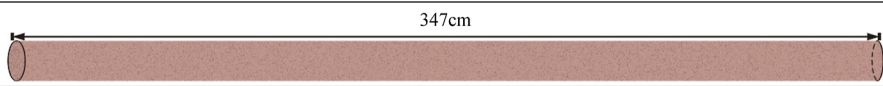


Figure 1. Research area and sampling schematic: (A) Geological map of the Chishui area. (B) Satellite image of the study area. (C) Sampling schematic.

This review summarizes important weathering indices from chemical and mineralogical aspects and discusses their limitations and usefulness. In general, weathering indices are considered the most useful solution to evaluating the weathering degree for particular purposes.¹³ Based on the study of existing

weathering indices and local weathering characteristics, our team mentioned that iron ions in red sandstone do not easy to migrate. The iron ion valence and content changes are mainly caused by surface oxidation. Therefore, the weathering degree can be studied using iron ion weathering-sensitive properties,

Table 1. Sample Test Arrangement



Iron ion content test	Powder samples were ground at 2.5cm intervals within 0-30cm; 30-80cm with 5cm interval grinding powder sample; 80-110cm with 10cm interval grinding powder sample; Deeper depth grinding powder samples at intervals of 15 cm.
Physical properties test	The standard sample was prepared by dividing the core by 10 cm. It measures the wave velocity, density, Leeb hardness, resistivity, and water absorption value at different depths.
Microstructure and Mineral	The powder samples were ground at depths of 5cm, 10cm, 15cm, 20cm, 35cm, 55cm, 80cm, 110cm, 145cm, and 164cm.

which is Fe^{2+} are easy to oxidize and Fe^{3+} are difficult to migrate. Iron ion relative weathering index (IRWI), a new weathering index, was established. The interrelationships between the iron ions and the changes in mineral composition and physical indicators were studied, and their conformity was discussed. Microstructural observation and pore distribution tests further verify the feasibility of evaluating red sandstone using the weathering index.

2. FORMER WORK ON WEATHERING INDICES

The chemical weathering index has attracted researchers' attention since the last century due to its quantifiable characteristics. Based on the changes in the chemical content of rock before and after weathering and the relationship with weathering degree,^{13,14} more than 20 chemical weathering indices have been proposed.^{15,16} Among earlier traditional chemical weathering indices, the "chemical index of alteration (CIA)" identifies the weathering degree by the alteration of feldspar. The larger the value of CIA, the greater the degree of weathering of feldspar in clay minerals, indicating the loss of potassium, calcium, and sodium in the parent rock. However, changes in iron, magnesium, phosphorus, and other elements are not considered. It should be assumed that the aluminum remains the same in the weathering process, which is difficult to fulfill the conditions in practice and is not applicable to sedimentary rocks of clastic and authigenic calcite.¹⁷ In contrast, the "chemical index of weathering excluded CaO (CIX)" is more suitable for determining the weathering degree of the sedimentary rocks containing clastic and other rocks because the influence of calcium oxide does not need to be considered, which makes up for the shortcomings of the CIA. The rest of the limitations are the same as those of the CIA.¹⁸ "Plagioclase index of alteration (PIA)" reflects the weathering degree based on the alteration of plagioclase in silicate rocks, and its limitations are similar to those of CIA. Still, it excludes the effect of K_2O , so it is not sensitive to the weathering of potassium feldspar-rich rocks.¹⁹ "Index of chemical variation (ICV)" mirrors the proportion of aluminum or clay minerals in the detrital rocks to other components, which is determined by the ratio of the sum of the easy-to-migrate elements and hard-to-migrate aluminum. However, it is high in easily weathered rock minerals such as pyroxene and hornblende, and low in relatively stable rock minerals such as montmorillonite and kaolinite.²⁰

Hu et al.²¹ established plagioclase dissolution rate (Nf) based on the unstable and easy weathering of plagioclase, a main rock-forming mineral in granite, and statistically captured and analyzed the images of plagioclase dissolution rate under the microstructure. Although plagioclase is very sensitive to weathering, residuals are characterized by different degrees of weathering degrees. The plagioclase dissolution rate does not

apply to all granite weathering zones. Li et al.²² proposed the concept of maturity to classify the weathering degree by describing and analyzing the nature of microfracture and secondary alteration of feldspar minerals in weathered rocks, which resulted in the value of maturity ranging from 1.0 to 2.0, and that the larger the value, the higher the weathering degree. Due to the limitation of technical means at that time, a microscope is needed to be used for calculating maturity, and the alteration of minerals on the rock surface needed to be described, which brought a subjective effect.²³ Moreover, there were fewer indices to compare and correlate with the degree of maturation. Wu explored the accuracy of chemical weathering indices, such as CIA, MIA, CIW, CIX, and STI, on the discernment of the weathering degree of black shale, and established a discriminative function of principal elements affecting the weathering degree of black shale.²⁴ However, the determined weathering index W was verified only in a single geological profile, and its applicability needs further exploration. Liu et al.¹⁴ explored the effects of chemical weathering indices (WI, WPI, and LOI) proposed by the previous researchers on the weathering of ancient architectural stone elements and compared the monotonicity and sensitivity of each weathering index in indicating weathering in terms of weathering degree, depth, and time. The research results indicated that the weathering depth obtained from the results of the on-site penetrating-wave test (CT) was the same as that determined by chemical weathering indices. The basic principle of determining a chemical weathering index is that the index should vary monotonically with the weathering degree, time, and depth.

At present, there is a lack of study of the classification and quantitative evaluation of the weathering degree of red sandstone. The commonly used chemical weathering index indicates the change of weathering degree, mainly based on the hydrolysis reaction of silicate minerals and the component loss and enrichment thus caused. The weathering of rocks generally occurs in the unsaturated zone with poor leaching conditions. Even if rocks are obviously weathered, elements are generally not significantly leached or enriched,^{25–27} which leads to the ambiguous delineation of weathering zones, so it is necessary to select more sensitive elements to study the weathering of red sandstone. The visual red color of red sandstone is caused by the control of surface-attached cementation and matrix.²⁸ The color difference is mainly affected by the relative content between Fe^{2+} and Fe^{3+} .²⁹ Iron is its characteristic element, featuring weak migration and an easy-to-change valence state. Previous researchers propose to study weathering degree using the silica-aluminum–iron coefficient of residual accumulation and the maturity index.^{30,31} However, the enrichment rule of Fe_2O_3 in the weathering process is mainly adopted, while the oxidation of Fe^{2+} , which is a sensitive characteristic, is ignored. Some

scholars' have made up for such deficiency by exploring the weathering of isolated rocks based on the characteristics of iron ions that are easy to oxidize.³² However, Fe^{2+} needs to be in high content and easy to oxidize in the existing test method, making it challenging to satisfy the requirements for determining trace amounts of Fe^{2+} . Plus, the signal of the change of Fe^{2+} is not sensitive. Thus, the determination of Fe^{3+} was also affected, making the established weathering index poorly indicated.

3. SAMPLE AND METHOD

3.1. Sample Preparation and Test Planning. The red sandstone used in this paper was sampled from the natural giant thick-bedded red sandstone slopes of the second section of the Jiading Group in a quarry in Chishui, Guizhou. The research area and the rock core are, respectively, shown in Figure 1 and Table 1.

To comprehensively evaluate the weathering degree and validate the IRWI indication effect from multiple perspectives, the test was designed to be divided into three sections, namely, iron ion content test, physical indicator test, and mineral composition, and microstructure test.

- (1) Iron ion content test: the improved *o*-phenanthroline spectrophotometric method determined the contents of Fe^{2+} and Fe^{3+} at different core depths. The above method involves several steps, namely, digestion, capacity determination, color reaction, and colorimetric, which are described explicitly at Text S1.
- (2) Physical test: According to the Standard for Testing Methods of Engineering Rocks (GB/T50266-2013), sample preparation requirements, and test standards were carried out to test the longitudinal wave velocity, density, resistivity, Leeb hardness, and water absorption of weathered rocks at different depths. More test details are given at Text S2.
- (3) Mineral composition and microstructure test: Mineral composition was analyzed by X-ray diffraction (XRD), microstructure were observed by scanning electron microscopy (SEM), and pore distribution was tested by nuclear magnetic resonance (NMR). Test instruments and procedures are described at Text S3.

3.2. Characterization of Iron Ion Alteration. The Fe^{2+} , Fe^{3+} , and total iron contents at different depths were determined according to the above method and plotted as a function of depth, as shown in Figures 2 and 3.

As can be seen from Figures 2 and 3, Fe^{2+} and Fe^{3+} contents in red sandstone showed prominent weathering sensitivity with depth changes, Fe^{2+} was positively correlated as a whole, and Fe^{3+} was negatively correlated as a whole, which could be utilized to study the weathering differences at different depths and to delineate the weathering degree by using the ratio between the two.

As can be seen from Figure 2, the change curve of Fe^{2+} content showed a V-shaped trend, first decreasing, then increasing, and finally stabilizing approximately at a fixed value. Fe^{2+} content was in the depth of 0–30 cm and because of shallow burial depth, weathering factors (water, temperature) continued to maximize the effect of calcium cement in the surface red sandstone, dissolution, feldspar, and other minerals eroded into clay and washed away. Therefore, in the same unit of mass, the proportion of iron cement, quartz, and other silicate minerals on the surface of red sandstone rose sharply. Hence, the enhancement rate of Fe^{2+} was greater than the oxidation rate in

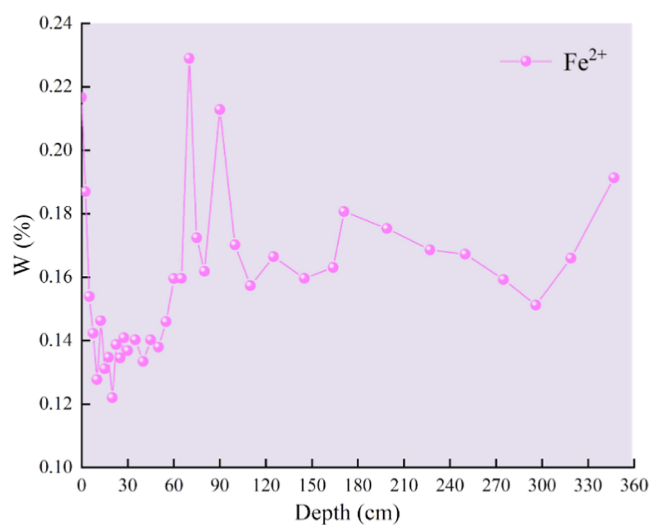


Figure 2. Fe^{2+} vs depth.

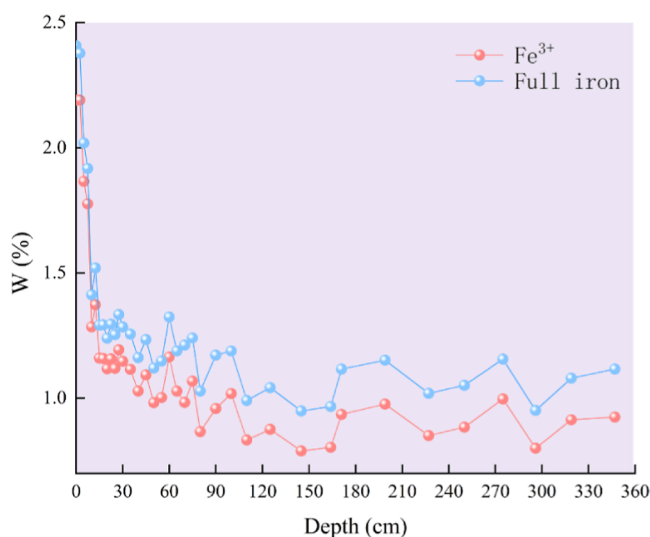


Figure 3. Fe^{3+} vs depth.

the surface endowment, causing the Fe^{2+} content in the surface weathering to remain at a high value. When the depth was in the range 30–70 cm, the buried depth was relatively large, the influence of Fe^{2+} by rainfall was relatively tiny, and it merely relied on O_2 to gradually oxidize Fe^{2+} to Fe^{3+} through the pore space generated by thermal stress and rainwater infiltration. Therefore, the content of Fe^{2+} noticeably increased with depth. When the depth at >70 cm, weathering factors such as rainfall and sunlight exerted a more limited effect on the red sandstone. The Fe^{2+} content reached a relatively high value, fluctuating up and down within a range.

As can be seen from the graph of Fe^{3+} change with depth, the change curve of Fe^{3+} (all iron) content differs from that of Fe^{2+} , showing a more pronounced and continuous downward trend and finally converging to a fixed value. However, the decreasing amplitude varied at different burial depths. When the depth was 0–30 cm, the change trend was similar to that of the Fe^{2+} content, mainly caused by the more severe weathering of the surface layer affected by rainfall scouring. The closer to the surface of the rock body, the more serious the rainfall scouring. Under the same unit mass, the proportion of iron cement, quartz, and other silicate minerals in the red sandstone

increased, and the Fe^{3+} (all iron) content increased. At the same time, the sensitivity of Fe^{3+} (all iron) led to a remarkable decrease in its content with the increase in depth, showing a steep decline. When the depth was in the range of 30–70 cm, contrary to the change of Fe^{2+} content, Fe^{3+} (all iron) content still slowly declined, which was related to the increase of burial depth. The depth of rainfall impact was limited, mainly relying on the penetration of rainfall, the role of thermal stress irradiation, and weathering effect was not vigorous and weathering was not intense. On the other hand, the proportion of iron cement and silicate minerals are slowly increased. When the depth at >70 cm, Fe^{3+} (all iron) content reached a relatively low value and changed smoothly because of the small influence of weathering. Its change was consistent with the Fe^{2+} content, which fluctuated within a specific range.

3.3. Degrees of Weathering. Based on the above research, the relative weathering index of iron ions is established and determined by the following formula.

$$\text{IRWI} = W_{(\text{Fe}^{3+})} / W_{(\text{Fe}^{2+})}$$

where $W_{(\text{Fe}^{3+})}$ is the mass percentage of Fe^{3+} and $W_{(\text{Fe}^{2+})}$ is the mass percentage of Fe^{2+} . From this formula, the IRWI versus depth curve is plotted. Therefore, the closer to the surface is, the stronger the oxidation, resulting in a large relative proportion of Fe^{3+} . Simply, the larger the IRWI value, the higher the weathering degree.

As can be seen from Figure 4, the absolute value of the slope of the weathering index curve was relatively large when depth at 0–

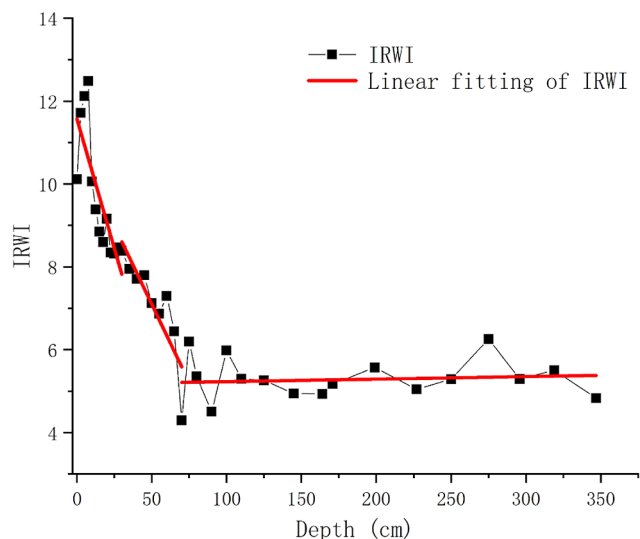


Figure 4. IRWI vs depth.

30 cm, indicating that the elemental content changed significantly in this depth range and that the red sandstone was most seriously affected by weathering; when the depth is in the range of 30–70 cm, the slope of the curve decreased, indicating that the weathering exogenic force continued to weaken and the weathering influence gradually decreased in this depth range. When depth at >70 cm, the curve trend suddenly changed into an approximate straight line. This indicates that after this depth, the influence of weathering exogenic force effect was slight, and elemental change was insignificant. With the weakening of the weathering degree, the Fe^{2+} content increased, while the Fe^{3+} content gradually decreased, with a gradual decrease in the ratio between the two and noticeable difference

in the ratio at different depths. The curve characteristics of IRWI with depth in the figure are summarized as steep decline, gradual change, and smooth fluctuation. Therefore, the shallow weathering zone of red sandstone was divided into a strong weathering zone with a depth of 0–30 cm, a medium weathering zone with a depth of 30–70 cm, and a slight weathering zone with a depth of >70 cm.

The IRWI based on the above understanding of the weathering sensitivity of iron ions highlights the indicative role of Fe^{2+} , reflecting the sensitivity of Fe^{2+} to oxidation during weathering. Spectrophotometry can be used to quantitatively analyze the components to be measured by determining the absorbance of sample at a specific wavelength, which has the advantages of noninterference with the components to be measured, low limit of detection, easy operation, etc. It is especially suitable for detecting trace iron ion content in red sandstone.^{33–35} Rock weathering is affected by many factors, including climate environment, geological structure, lithology, topography, and geomorphology.³⁶ Under the combined influence of many factors, the method will inevitably have regional limitations in determining the weathering degree.³⁷ In addition, the improved phenanthroline spectrophotometric method in this paper can determine only the iron content in red sandstone, and it is temporarily impossible to further analyze Fe^{2+} and Fe^{3+} in different occurrence states (cement, mineral lattice, and mineral surface film) in red sandstone. For the iron ion determination, the effect of sample digestion and color development greatly depends on the type and ratio of chemical agents. It is essential to select the appropriate digestion solution and digestion time to ensure that Fe^{2+} is not disturbed and all is extracted, which is also the main content of the improvement of phenanthroline spectrophotometry in this paper.

4. PHYSICAL WEATHERING CHARACTERISTICS OF RED SANDSTONE

4.1. Characteristics of Physical Indicators of Each Weathering Zone. To better characterize the correlation between each physical indicator and IRWI, the magnitudes of longitudinal wave velocity, Leeb hardness, density, resistivity, and water absorption at different depths of the red sandstone were measured according to the rock test standard. The linear fitting of each physical indicator with depth change was established to more intuitively observe the physical characteristics at each stage and the correlation with IRWI.

As shown in Figure 5a,b, at a depth of 0–30 cm, red sandstone's drying and saturation wave velocity steeply increased, the weathering showed apparent attenuation, and the erosion slowed down with the increase in depth. The number of pores and fissures in the red sandstone also declined. At a depth of 30–70 cm, the drying and saturation wave velocity of the red sandstone exhibited a gradual rise, and weathering was mainly by infiltration. The number of pores and fissures in the red sandstone slowly decreased. At a depth of >70 cm, red sandstone's dry and saturated wave velocity fluctuated gently within a specific range. Therefore, the linear fitting of longitudinal wave speed was negatively correlated with IRWI's.

The drying and saturated Leeb hardness values at different depths are shown in Figure 5c,d. There were significant differences at a depth range of 0–30 cm. The drying and saturated Leeb hardness values increased sharply with the increase in depth. The growth magnitude of the drying and saturated Leeb hardness values decreased when the depth was 30–70 cm, while that stabilized at a depth of >70 cm. Therefore,

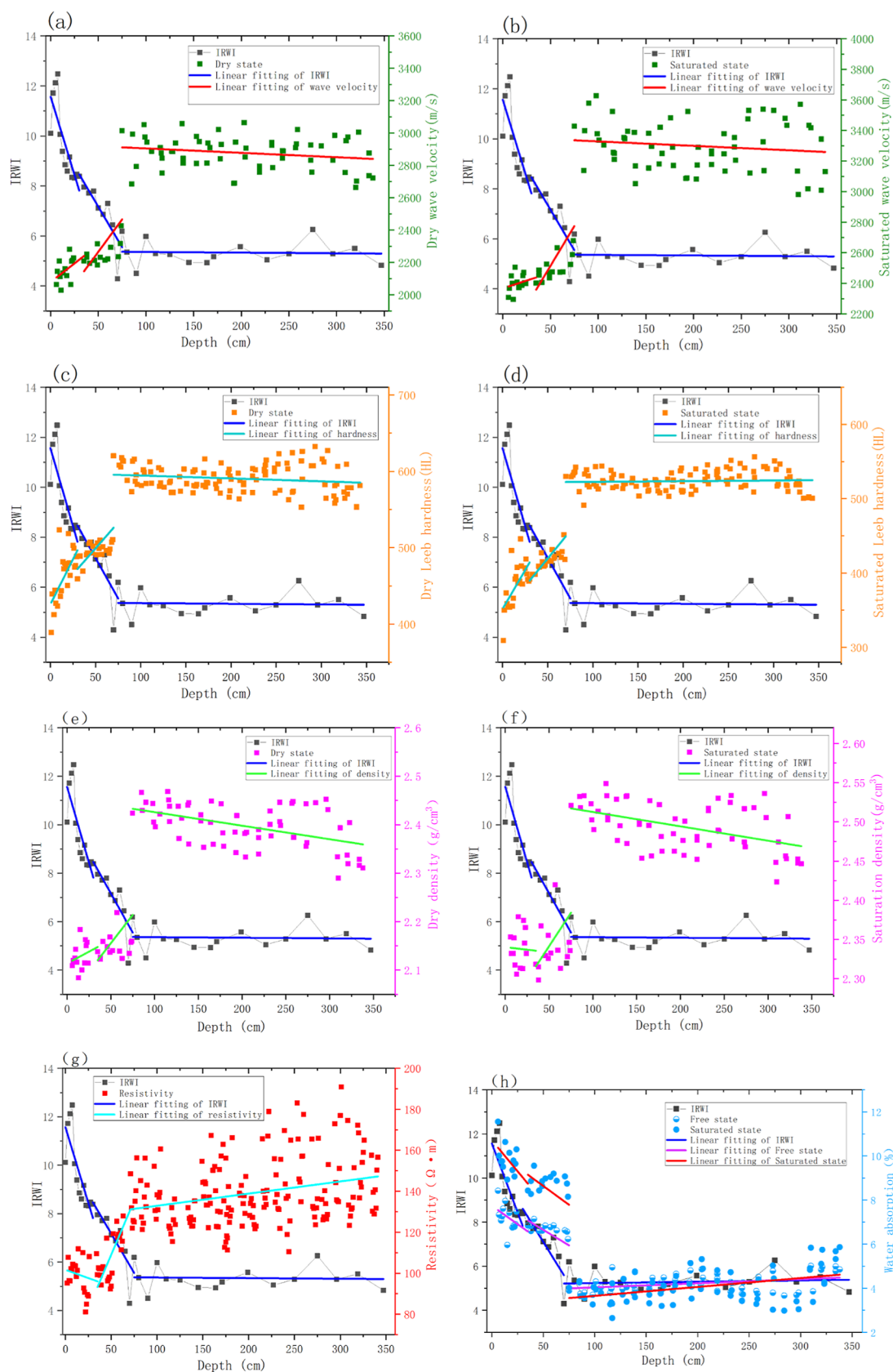


Figure 5. Correlation of the physical indicators with IRWI. (a) Linear fit of dry wave velocity; (b) linear fit of saturated wave velocity; (c) linear fit of dry Leeb hardness; (d) linear fit of saturated Leeb hardness; (e) linear fit of dry density; (f) linear fit of saturated density; (g) linear fit of resistivity; and (h) linear fit of water absorption.

the linear fitting of Leeb hardness was negatively correlated with that of IRWI.

Figure 5e,f shows that the dry and saturated densities at a depth of 0–30 cm were maintained in a relatively stable interval and did not significantly increase with the weakening of the weathering degree, that at a depth of 30–70 cm showed a gradual upward trend, and that at a depth of >70 cm fluctuated stably, with a clear demarcation point between strong weathering and medium weathering. Therefore, the linear fit of density was closely negatively correlated with that of IRWI.

Figure 5g shows significant differences in resistivity at different depths. At a depth of 0–30 cm, the resistivity value fluctuated with the increase in depth, indicating that severe weathering, many pores and fissures within the red sandstone were extensive, and a high degree of openness. At a depth of 30–70 cm, the resistivity values show an overall increasing trend with depth, indicating that weathering gradually decreases within this depth as a transition zone. The number of pores and fissures as well as the degree of opening within the red sandstone, is gradually decreasing. The resistivity value tended to stabilize with the increase of the depth at a depth of >70 cm, peaking in this range, which indicates that the influence of weathering was small in this depth and that the number of pores and fissures and degree of opening in the red sandstone were roughly similar. Therefore, the overall linear fit of resistivity was negatively correlated with that of IRWI.

As shown in Figure 5h, the red sandstone's free and saturated water absorption rate showed a steep decline. At a depth of 0–30 cm, weathering became weaker with the depth increase, and erosion slowed down so that the number of pores, fissures, and the degree of opening were gradually reduced. At a depth of 30–70 cm, the water absorption rate gradually declined, and the decrease of the pore rate was mainly dominated by large open pores. The number of pores and fissures decreased slowly, mainly due to the decrease in the degree of pore opening. At a depth of >70 cm, the water absorption rate fluctuated gently within a certain range, and the external weathering factor had a slight effect. The number, size, and degree of opening of pores and fissures in the red sandstone were mainly influenced by a rock-forming environment. The change in water absorption rate indirectly reflects that the change of internal pores with depth, indicating that the weathering of red sandstone was closely related to IRWI.

4.2. Mineral Composition Analysis. In nature, major rock-forming minerals, in descending order of resistance to weathering, are calcite, olivine, calcium feldspar, pyroxene, hornblende, sodium feldspar, smectite, potassium feldspar, muscovite, clay minerals, quartz, and oxides of aluminum and iron. Weathering often results in the transformation of unstable minerals into stable minerals. The results are shown in Table S1 and Figure 6.

As can be seen from Figure 6, minerals in the red sandstone were mainly quartz, feldspar, calcite, hematite, and clay, and their percentage contents varied among depths. With the increase of depth, the content of quartz, potassium feldspar, clay, hematite, and other major minerals gradually decreased in the order of clay > hematite > quartz > potassium feldspar. In contrast, plagioclase and calcite gradually increased in the order of calcite > plagioclase.

In the strong weathering zone, calcite was basically dissolved in red sandstone. Plagioclase and potassium feldspar have relatively weak weathering resistance. They undergo different alterations to form clays. Plagioclase was significantly dissolved

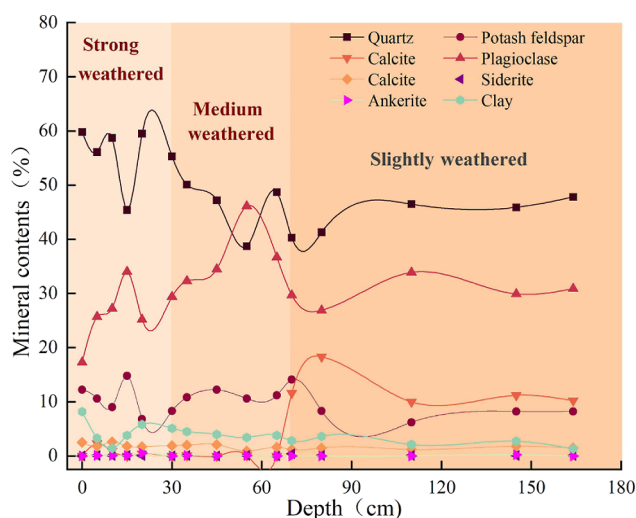


Figure 6. Mineral content with depth.

as a characteristic of the change, which resulted in the increase in the content of quartz, clay, and hematite and weathering resistance. In the medium weathering zone, the content of plagioclase increased significantly, with the average content rising from 26.47 to 37.4% that in the strong weathering zone, but the content of calcite was still nearly 0%. The content of minerals with strong weathering resistance, such as quartz, clay, and hematite, is greatly reduced. In the slightly weathering zone, the content of calcite, a mineral easy for weathering, increased significantly, with an average content of 12.26%, which indicated that the weathering degree was significantly different from that in the strong and medium weathering zones, corresponding to the fact that the red sandstone powder in the slightly weathered zone can produce a certain amount of CO₂ bubbles when encountering acid in the determination of iron ions content.

4.3. Microstructure Analysis. To further investigate the effect of weathering on the microscopic scale of the red sandstone, the microstructure and pore distribution of the three weathered sandstones were tested and analyzed separately.

4.3.1. Cementation and Microstructure. The cement and microstructure were observed by SEM, as shown in Figure 7.

It can be seen from Figure 7, that the microstructure of red sandstone in the strong weathering zone is seriously broken, and honeycomb dissolution pores appear in quartz particles. Due to the development of pores, the cementation between particles becomes loose, and many cements have been lost. Red sandstone in the medium weathering zone had a relatively good microstructure, the surface of the quartz particles was broken, dissolution pits and interparticle fissures were relatively well developed, and a certain number of cement was lost. Red sandstone in the slightly weathered zone owned a complete microstructure with a smooth surface of quartz grains, occasional fissure development, and well-preserved cement.

4.3.2. Characteristics of Pore Distribution. The red sandstone was tested using an NMR analyzer, resulting in T2 spectra, pore size distributions, and pore throat distributions, as shown in Figures 8, 9, and 10.

As can be seen from the T2 spectra, there were two prominent peaks on the T2 spectral curve, one in the range of 0.03–4 ms and the other in the range of 4–200 ms, corresponding to small and large pores, respectively. With the increase of weathering intensity, the T2 spectral curve shifted to the right, and the peak area increased gradually, indicating that the size and number of

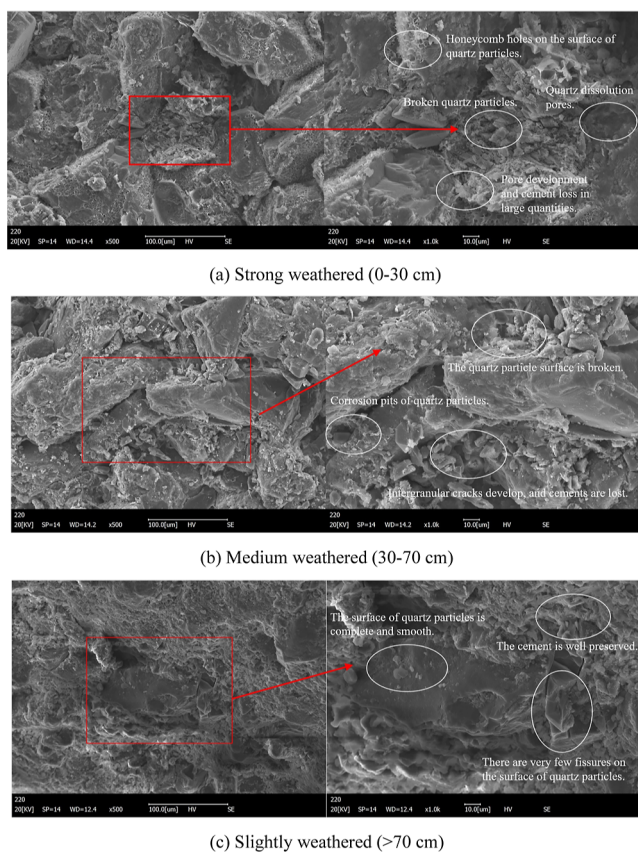


Figure 7. Microstructure of red sandstone with different weathering degrees.

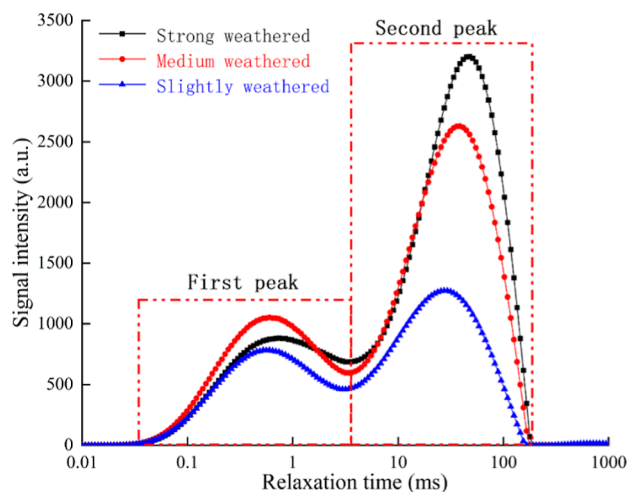


Figure 8. T₂ spectrum.

pores inside the rock increased gradually. The T₂ spectra of the strongly weathered zone (0–30 cm) and the medium weathered zone (30–70 cm) had similar areas and peaks as well as similar distribution of pore situation and pore number per unit volume. In comparison, the difference in the distribution of slightly weathered zone (>70 cm) was noticeable, which indicates that weathering zones were reasonable.

According to the pore size ratio and distribution [Figure 9](#) and [Table 2](#). Weathering degraded the pore structure, which was mainly characterized by the increase of the pore number and pore size. According to the percentage of pore size, the pore size

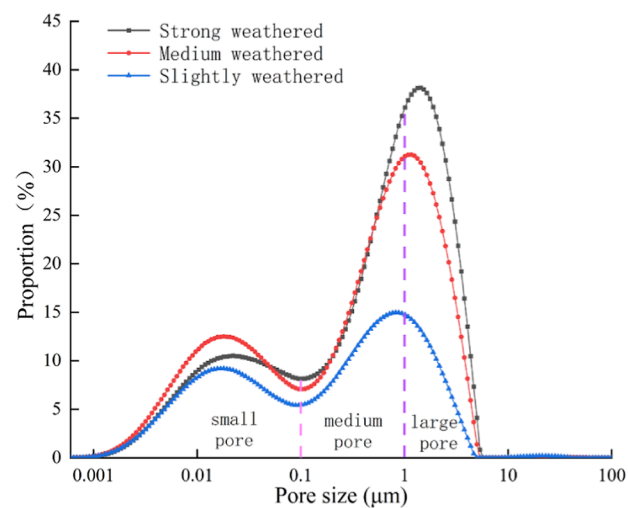


Figure 9. Pore size distribution.

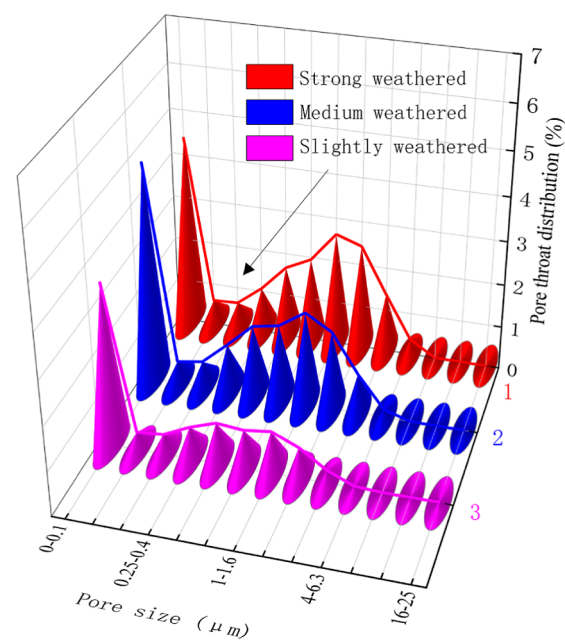


Figure 10. Average pore throat distribution.

Table 2. Percentage of Pore Size Distribution with Different Weathering Degrees

degree of weathering	small pore (%)	medium pore (%)	large pore (%)
strong	25.63	34.53	39.84
medium	31.56	36.14	32.3
slightly	40.12	37.86	22.02

of the red sandstone was divided into three categories: small pore (pore size < 0.1 μm), medium pore (pore size of 0.1–1 μm), and large pore (pore size > 1 μm), and with the increase of weathering degree, the percentage of small pore decreased from 40.12% in the slightly weathered to 25.63% in the strongly weathered, and that of large pore increases from 22.02% in the slightly weathered to 39.84% in the strongly weathered. It indicates that the deterioration of the microstructure of the red sandstone by weathering is a gradual process accompanied by the generation and expansion of pores.

Pore throat refers to the interconnected channels between pores. The larger the pore throat, the stronger the permeability, the more conducive it is to material exchange between pores, and the greater the degree of weathering impact. According to Figure 10, pore throats ranging from 0 to 0.1 μm had the largest proportion, followed by pore throats ranging between 1 and 1.6 μm . The overall trend appeared to be wavy, with the degree of fluctuation closely related to the extent of weathering. As rock weathering weakened, the distribution curve of pore throats gradually fluctuated more and more gently. Notably, the most significant changes in the distribution curve emerged between microweathering and other weathering degrees.

5. CONCLUSIONS

- (1) The improved *o*-phenanthroline spectrophotometry was used to determine the red sandstone samples, in which the Fe^{2+} content first decreases and then increases with depth and finally converges to a constant value. The change curve of the Fe^{3+} (all iron) content shows a more obvious downward trend and the ultimate convergence to a constant value, but decreasing amplitude varies at different burial depths. According to the relationship between IRWI and depth, the shallow weathering zone of Chishui red sandstone is divided into a strong weathering zone (0–30 cm), medium weathering zone (30–70 cm), and slightly weathering zone (>70 cm). Combined with the analysis of IRWI in Section 3.2, the red sandstone IRWI values can be determined as strongly weathered when it is greater than 8.3, as medium weathered when it is 8.3–6.4, and slightly weathered when it is 6.4–4.5.
- (2) Through a series of studies on the variation characteristics of physical indicators with depth, including density, porosity, wave velocity, Richter hardness, and resistivity, the physical indicators are consistent with the corresponding weathering degree, and have obvious correlation and sensitivity with IRWI.
- (3) The mineral composition analysis results show that the strong weathering zone of red sandstone is mainly characterized by the significant dissolution of calcite and plagioclase, medium weathering zone by the basic dissolution of calcite and a significant increase in plagioclase content, and a slight weathering zone by a significant increase in calcite. The microstructural observation and pore distribution of each weathering zone were analyzed separately, and the results validate the differences in the microstructure under weathering zones after IRWI division.

This study provides a new methodological framework for evaluating the weathering degree of red-layer sandstone, a technical means for further in-depth study of the weathering mechanism in the red bed area of Chishui and theoretical support for the study of coloration mechanism, environmental redox changes, and the protection of sandstone rock carvings and cultural relics in the red bed area.

■ ASSOCIATED CONTENT

SI Supporting Information

The Supporting Information is available free of charge at <https://pubs.acs.org/doi/10.1021/acsomega.3c07417>.

Test procedure of *o*-phenanthroline spectrophotometry, test procedure of the physical indicator, mineral and

microstructure test, and change of the mineral composition with depth are detailed (PDF)

■ AUTHOR INFORMATION

Corresponding Authors

Saidong Li – College of Resources and Environmental Engineering, Guizhou University, Guiyang 550025, China; orcid.org/0009-0006-5895-2946; Email: saidongli@foxmail.com

Genlan Yang – Key Laboratory of Karst Geological Resources and Environment, Ministry of Education, Guizhou University, Guiyang 550025, China; Email: 251491904@qq.com

Authors

Wenjie Jiang – Key Laboratory of Karst Geological Resources and Environment, Ministry of Education, Guizhou University, Guiyang 550025, China

Xiqiong Xiang – Key Laboratory of Karst Geological Resources and Environment, Ministry of Education, Guizhou University, Guiyang 550025, China

Chongping Huang – Key Laboratory of Karst Geological Resources and Environment, Ministry of Education, Guizhou University, Guiyang 550025, China

Complete contact information is available at:

<https://pubs.acs.org/10.1021/acsomega.3c07417>

Notes

The authors declare no competing financial interest.

■ ACKNOWLEDGMENTS

This study was supported by Guizhou Provincial Basic Research Program (Natural Science) -ZK [2021] Basic 200. The authors thank Chongping Huang and Dajuan Wang for their help in the sample collection and test data analysis processes.

■ REFERENCES

- (1) Turkington, A. V.; Paradise, T. R. Sandstone weathering: a century of research and innovation. *Geomorphology* **2005**, *67* (1–2), 229–253.
- (2) Vidana Pathiranagei, S.; Gratchev, I.; Cui, C.; Elmore, B. New weathering classification system of rocks based on the engineering properties. *Bull. Eng. Geol. Environ.* **2023**, *82* (2), 60.
- (3) Zhang, K.; Liu, R.; Bai, E.; Zhao, Z.; Peyrotty, G.; Fathy, D.; Chang, Q.; Liu, Z.; Yang, K.; Xu, C.; Liu, Z. Biome responses to a hydroclimatic crisis in an Early Cretaceous (Barremian–Aptian) subtropical inland lake ecosystem, Northwest China. *Palaeogeography* **2023**, *622*, 111596.
- (4) Monticelli, J. P.; Sígolo, J. B.; Futai, M. M. On weathering understanding and its characterization by petrographic indices: a study case about the criterion establishment for the textural classification of rock-forming minerals under weathering. *Environ. Earth Sci.* **2021**, *80* (11), 408.
- (5) Topal, T. Quantification of weathering depths in slightly weathered tuffs. *Environ. Geol.* **2002**, *42* (6), 632–641.
- (6) Aldred, J.; Eppes, M. C.; Aquino, K.; Deal, R.; Garbini, J.; Swami, S.; Tuttle, A.; Xanthos, G. The influence of solar-induced thermal stresses on the mechanical weathering of rocks in humid mid-latitudes. *Earth Surface Processes and Landforms* **2016**, *41* (5), 603–614 (in Chinese with English abstract).
- (7) Collins, B. D.; Stock, G. M.; Eppes, M. C.; Lewis, S. W.; Corbett, S. C.; Smith, J. B. Thermal influences on spontaneous rock dome exfoliation. *Nat. Commun.* **2018**, *9*, 762.
- (8) Lamp, J. L.; Marchant, D. R.; Mackay, S. L.; Head, J. W. Thermal stress weathering and the spalling of Antarctic rocks. *J. Geophys. Res.: Earth Surface* **2017**, *122* (1), 3–24.

- (9) Leng, Y. Y.; Luo, B. J.; Zhang, L.; Yang, L. The destructive effect of Chishui Danxia caused by rock body temperature stress and differentiating weathering. *Guizhou Geol.* **2017**, *34* (02), 123–127. (in Chinese with English abstract)
- (10) Zhong, K.; Liu, A.; Xie, Q. Investigation and experimental study on weathering and spalling process of red layer slope. *Roadbed Eng.* **2000**, *4* (4), 53–56. (in Chinese with English abstract)
- (11) Tan, Y. F.; Li, L. H.; Yang, Z. F.; Liao, X. H. Moisture stress effect and its control on differential weathering of red-bed sandstone and conglomerate. *J. Rock Mech. Eng.* **2019**, *38* (S2), 3481–3492. (in Chinese with English abstract)
- (12) Zhang, B.; Cheng, W.; Zhang, Q.; Li, Y.; Sun, P.; Fathy, D. Occurrence Patterns and Enrichment Influencing Factors of Trace Elements in Paleogene Coal in the Fushun Basin, China. *ACS Earth Space Chem.* **2022**, *6* (12), 3031–3042.
- (13) Wu, H. W.; Shang, Y. J.; Qu, Y. X.; P, M. B. Chemical index system for weathering grading and weathering crustal zoning of Hong Kong granites. *J. Eng. Geol.* **1999**, *7* (02), 29–38. (in Chinese with English abstract)
- (14) Liu, C. Y.; He, M. C. Method of Determining Weathering Depth of Rock Ancient Building. *J. Earth Sci. and Environ.* **2008**, *30* (1), 69–73. (in Chinese with English abstract)
- (15) Gupta, A. S.; Rao, S. K. Weathering indices and their applicability for crystalline rocks. *Bull. Eng. Geol. Environ.* **2001**, *60* (3), 201–221.
- (16) Liu, C. Y.; He, M. C. A study of chemical weathering indices sensitive to the degree of rock weathering. *Earth Environ.* **2011**, *39* (3), 349–354. (in Chinese with English abstract)
- (17) Nesbitt, H. W.; Young, G. M. Early Proterozoic climates and plate motions inferred from major element chemistry of lutites. *Nature* **1982**, *299*, 715–717.
- (18) Garzanti, E.; Padoan, M.; Setti, M.; Lopez-Galindo, A.; Villa, I. M. Provenance versus weathering control on the composition of tropical river mud (southern Africa). *Chem. Geol.* **2014**, *366*, 61–74.
- (19) Fedo, C. M.; Wayne Nesbitt, H.; Young, G. M. Unraveling the effects of potassium metasomatism in sedimentary rocks and paleosols, with implications for paleo weathering conditions and provenance. *Geology* **1995**, *23*, 921–924.
- (20) Jayawardena, U. d. S.; Izawa, E. A new Chemical Index of Weathering for metamorphic silicate rocks in tropical regions: a study from Sri Lanka. *Eng. Geol.* **1994**, *36*, 303–310.
- (21) Hu, R.; Oyediran, I. A.; Gao, W.; Zhang, X. Y.; Li, L. H. "Plagioclase solution degree index": a new index to evaluate the weathering degree of granite. *Bull. Eng. Geol. Environ.* **2014**, *73* (2), 589–594.
- (22) Li, R.; Wu, L. F. Research on characteristic indices of weathering intensity of rocks. *Chin. J. Rock Mech. Eng.* **2004**, *23* (22), 3830–3833. (in Chinese with English abstract)
- (23) Zhang, L.; Zhang, J.; Guo, Q.; Wang, Y.; Huang, L. Quantitative assessment of weathering of cretaceous sandstone relics in Longdong Area from the surface to the interior. *Sediment. Geol.* **2022**, *441*, 106265.
- (24) Wu, B. J. Geochemical characteristics of weathered lower-cambrian black shales in central Hunan; China. Dissertation, Hunan Normal University, China, Hunan, 2016.
- (25) Xu, Z.; Huang, R. Q. The assessment of the weathering intensity of Emeishan basalt based on rock blocks (IV): A proposed weathering index (FF). *China Geol.* **2013**, *40* (6), 1942–1948. (in Chinese with English abstract)
- (26) Zhang, X. S. Expansion Mechanism of Weathering Front of Rock Blocks with Low Permeability in Slope Unsaturated Zone, Dissertation, Kunming University of Science and Technology, China, Kunming, 2017.
- (27) Tang, P. The temperature effect of rock structure weathering front expanding process under the non-saturated zone environment, Dissertation, Kunming University of Science and Technology: China, Kunming, 2008.
- (28) Tan, C.; Yu, B. S.; Yuan, X. J.; Liu, C.; Wang, T. S.; Zhu, X. Color Origin of the Lower Triassic Liujiagou and Heshanggou Formations Red Beds in the Ordos Basin. *Mod. Geol.* **2020**, *34* (04), 769–783. (in Chinese with English abstract)
- (29) Zhang, K.; Ma, M.; Ma, L.; Cai, M.; Li, Y. X. Determination of ferrous oxide in iron ore by potentiometric titration method. *Metall. Anal.* **2018**, *38* (05), 66–71. (in Chinese with English abstract)
- (30) Ma, X. C.; Wang, J. S.; Chen, C.; Wang, Z. Major Element Compositions and Paleoclimatic Implications of Paleo-Regolith on Top Jingeryu Formation in Fangshan, North China. *Earth Sci.* **2018**, *43* (11), 3853–3872. (in Chinese with English abstract)
- (31) Fu, H. J.; Jian, X.; Liang, H. H. Research progress of sediment indicators and methods for evaluation of silicate chemical weathering intensity. *J. Paleogeography* **2021**, *23* (6), 1192–1209. (in Chinese with English abstract)
- (32) Wang, D. J. Study on characteristics of red layer weathering in Danxia landform area, Chishui city, Dissertation, Guizhou University, China, Guizhou, 2020.
- (33) Zhang, X. H.; Dong, Y.; Zhang, L. Y.; Zheng, P. H.; He, L. F. Determination of micro cobalt(II) in water by 4-nitro-o-phenylenediamine-salicylaldehyde spectrophotometry. *Metall. Anal.* **2020**, *40* (9), 82–86.
- (34) Tian, L. F.; Dai, Y. C.; Zou, D. S. Spectrophotometric Determination of Small Amounts of Cadmium with Potassium Iodide and Rhodamine B. *Spectrosc. Spectral Anal.* **2018**, *38* (S1), 301–302. (in Chinese with English abstract)
- (35) Wu, X. S.; Xia, T.; Cen, C. G.; Chen, J. B. Determination of trace iron content by potassium ferrocyanide spectrophotometry. *Appl. Chem. Eng.* **2021**, *50* (7), 2022–2024. 2029 (in Chinese with English abstract)
- (36) Yao, R. Research of Carbon Sink Capacity Caused by Rock Weathering Process in China, Dissertation, Central South University, China, Hunan, 2003.
- (37) Matsuzawa, M.; Chigira, M. Weathering mechanism of arenite sandstone with sparse calcite cement content. *CATENA* **2020**, *187*, 104367.